



Experimental Validation of PSO and GWO-Based MPPT for a Single-Stage Three-Phase Grid-Connected PV System Under Partial Shading

Abdelmoumen Ghilani^{1*}, Amel Terki², Zakaria Alili³, Ahmed Marouane Ghodbane², Oussama Belaroussi²

¹ LMSE Laboratory, University of Biskra, Department of Electrical Engineering, Biskra 07000, Algeria

² LGEB Laboratory, University of Biskra, Department of Electrical Engineering, Biskra 07000, Algeria

³ LEE Laboratory, University of Msila, Department of Electrical Engineering, Msila 28000, Algeria

Corresponding Author Email: abdelmoumen.ghilani@univ-biskra.dz

Copyright: ©2024 The authors. This article is published by IETA and is licensed under the CC BY 4.0 license (<http://creativecommons.org/licenses/by/4.0/>).

<https://doi.org/10.18280/jesa.570514>

ABSTRACT

Received: 8 August 2024

Revised: 29 September 2024

Accepted: 10 October 2024

Available online: 28 October 2024

Keywords:

Grey Wolf Optimization, MPPT, Particle Swarm Optimization, partial shading conditions, PV grid-connected, single-stage topology

As global energy demands increase, grid-connected photovoltaic systems are gaining popularity and acceptance as a viable and attractive alternative energy source. These systems face significant challenges in terms of power quality and maximising solar panel output under varying environmental conditions. This study aims to experimentally validate the effectiveness and stability of a single-stage grid-connected photovoltaic system and to evaluate the performance of the Grey Wolf Optimization (GWO) and Particle Swarm Optimization (PSO) techniques in reaching the maximum power point under partial shading conditions. For experimental validation, dSPACE 1104 and LAUNCHXL-F28379D were used. The results demonstrate that the system exhibits both robustness and stability, with the GWO algorithm outperforming PSO in terms of speed and accuracy in achieving the maximum power point, thus enhancing the system's efficiency under different operating conditions.

1. INTRODUCTION

Electricity has become a crucial component in worldwide initiatives for economic and social development [1]. Therefore, renewable energy is a wise choice for producing environmentally friendly electricity without depending on conventional sources, which have finite supplies and significant ecological impacts. Solar energy is a prominent form of renewable energy because of its cleanliness, cost-efficiency, simplicity, and minimal maintenance needs, making it an optimal alternative for fulfilling energy requirements [2]. The widespread adoption of this technology is further facilitated by its ability to be used in a range of different sizes, from modest home systems to huge utility-scale facilities. With the ongoing advancement of technology, the effectiveness and cost-effectiveness of solar energy systems are anticipated to increase, hence strengthening their feasibility. Moreover, the incorporation of solar energy into current energy systems might enhance energy resilience [3].

The primary technical challenge of PV systems is their impoverished operational efficiency, which is caused by their nonlinearity in characteristics and the variability of weather conditions [2]. In order to maximise power output, it is necessary to develop algorithms that can accurately identify and track the maximum power point (MPP). These systems need to be efficient and accurate in identifying the maximum power point (MPP) and adapting to accommodate dynamic conditions. For many solar systems, the well-accepted methods of perturb and observe and incremental conductance are highly preferred and usually yield good results [4].

However, when panels are partially covered, these methods often encounter difficulties. Even as researchers explore other approaches like artificial neural networks and fuzzy logic control, these systems still struggle to maximise power generation under shadowed conditions [5].

A novel class of MPPT controllers based on metaheuristic approaches has become somewhat well-known recently. These techniques address the shortcomings of conventional MPPT systems and provide improved stability, thus more suited to fit evolving circumstances [1]. Originally intended for challenging optimisation issues in engineering and other domains, they find extensive use currently. Their ability to control difficult and nonlinear situations makes them fascinating. Metaheuristic algorithms shine in global optimisation; they ensure the real MPP within the operating range of the system [6].

Grid-connected solar systems typically use one of two main topologies. The first is the multi-stage system shown in Figure 1. This topology uses a DC-DC converter to monitor the maximum power point of the PV solar panel and increase its voltage [7]. In the second stage, an inverter synchronises and injects the PV power into the grid. This design was functional, but it had a lot of drawbacks, such as its huge size and high cost. Furthermore, the increased number of components and complex control systems result in higher initial costs, and upkeep expenses, power loss also escalates, thereby reducing the overall efficiency of energy transportation and potentially raising concerns about reliability. Additionally, there are concerns about subpar output quality and increased total harmonic distortion (THD) [8].

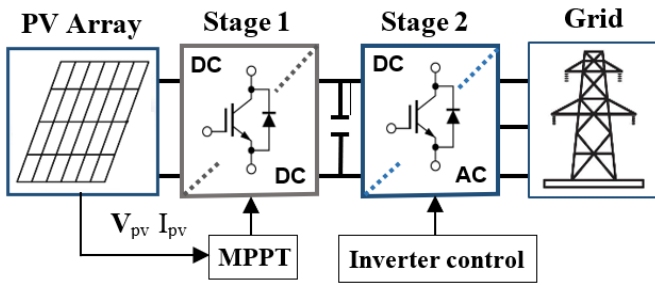


Figure 1. Multi-stage design

However, the second design shown in Figure 2 avoids the need for a DC-DC converter by directly linking the solar panels to an inverter that injects the photovoltaic electricity into the grid. This technique simplifies the system by decreasing its size, improving its efficiency, and maximising its cost-effectiveness [7]. This design enhances efficiency and streamlines the system by integrating the maximum power point tracking (MPPT) function directly into the inverter, hence reducing power losses. Furthermore, it offers improved reliability, streamlined installation, and less maintenance, making it a preferred choice for many photovoltaic systems [9].

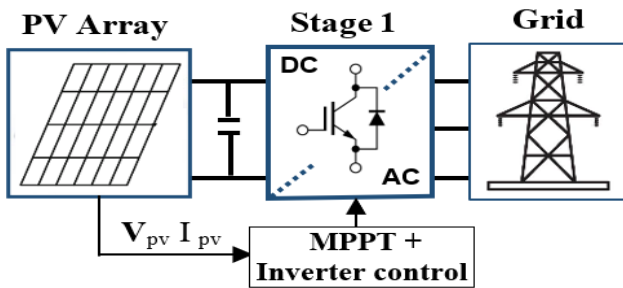


Figure 2. Single-stage design

The primary contribution of this paper is the practical validation of two metaheuristic-based MPPT techniques for single-stage, three-phase grid-connected photovoltaic systems under partial shading conditions. These techniques are PSO and GWO.

The objective is to utilise a single-stage system to validate that these two techniques can effectively track the maximum power point of the photovoltaic system under partial shading conditions. Additionally, it aims to ensure high-quality power injection and synchronisation with the grid.

The rest of the paper is organised as follows: Section 2 discusses the effects of partial shading on the PV system. Section 3 examines the control strategy of the single-stage PV grid-connected inverter. The details of the MPPT algorithms used are explained in Section 4. Section 5 encompasses the hardware description, results, and discussion of the single-stage, three-phase grid-connected PV systems. Section 6 presents this work's final conclusion.

2. IMPACTS OF PARTIAL SHADING ON THE PV SYSTEM

Obstacles such as trees, buildings, and clouds cause solar panels to be exposed to uniform or non-uniform solar radiation. During partial shading conditions (PSC), PV panels exposed to uneven solar radiation may consume power rather than generate it, leading to the formation of hotspots. To prevent

hotspots, each PV panel is fitted with a bypass diode connected in parallel. Additionally, a blocking diode is installed in series with each parallel string. As a result, there is a current mismatch among the series-connected PV panels and a voltage mismatch across the parallel-connected strings [10]. These mismatches produce many maximum power points (MPP) and distort the PV modules' power characteristics. Out of all these MPPs, the Global MPP (GMPP) is the highest; the others are called Local MPPs (LMPP). The physical arrangement of the PV modules and the weather conditions modify the positions of these MPPs [11].

In this study, the photovoltaic system comprises two solar panels connected in series. Figure 3 demonstrates that the presence of trees causes partial shading, resulting in uneven solar radiation exposure for numerous cells in these panels. The characteristics of the PV module utilised in this work are detailed in Table 1.



Figure 3. Photovoltaic panels utilised in this study

Table 1. PV module characteristics

The Parameter	The Value
Rated maximum power (P_{max})	190 W
Voltage at P_{max}	36.6 V
Current at P_{max}	5.69 A
Open-circuit voltage	85.3 V
Short-circuit current	6.09 A
The number of cells	128

To determine the photovoltaic characteristics of the panels, the LAUNCHXL-F28379D launchpad was used in conjunction with DC voltage and current sensors. As illustrated in Figure 4, partial shading results in the emergence of one Global Maximum Power Point (GMPP) at 191.7 W and two Local Maximum Power Points (LMPPs), specifically at 94.33 W and 67.54 W on the power-voltage (P-V) curve. The characteristic curves indicate that these shading conditions significantly impact the photovoltaic panel performance.

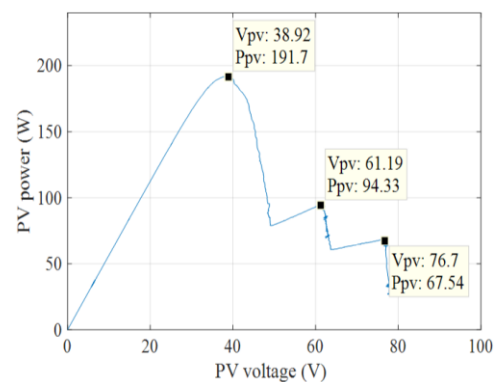


Figure 4. The power-voltage (P-V) characteristic curve

Figure 5 shows the corresponding current-voltage (I-V) behaviour under the same conditions, complicating the optimisation of energy extraction. As a result, it becomes essential to implement effective Maximum Power Point Tracking (MPPT) strategies.

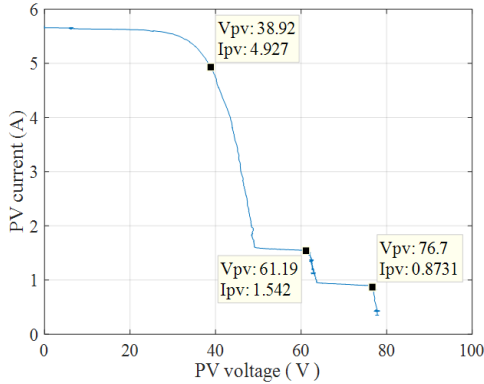


Figure 5. The current-voltage (I-V) characteristic curve

3. CONTROL STRATEGY OF THE SINGLE-STAGE PV GRID-CONNECTED INVERTER

In the single-stage topology, the inverter simultaneously injects photovoltaic power into the grid and tracks the maximum power point [12]. This means the inverter control is divided into two parts. The first part is responsible for tracking the maximum power point using tracking algorithms, as depicted in Figure 6. Following this, a proportional-integral (PI) controller ensures that the DC-link voltage equals the PV voltage reference V_{pvref} extracted by the MPPT algorithm. This loop generates the reference current peak value I_{max} [13]. The amplitude of the I_{max} current represents the active power that is injected into the grid and takes into consideration the losses in the system [14].

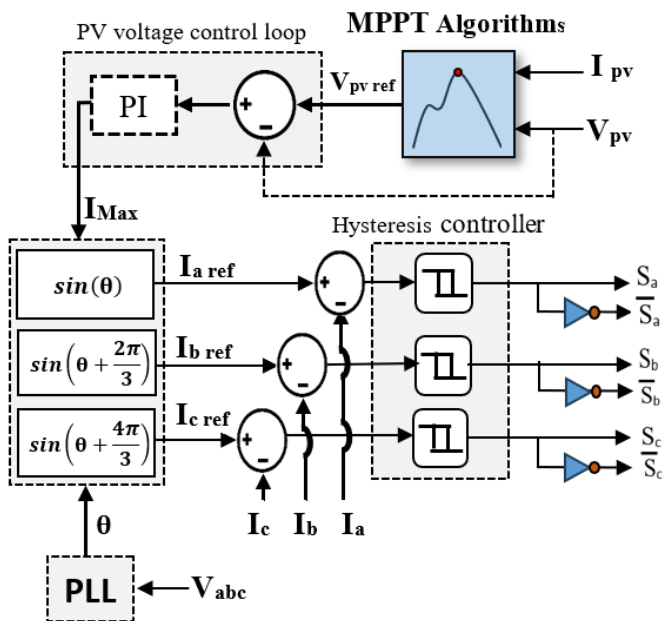


Figure 6. Control strategy for the grid-connected inverter

To ensure the inverter output is perfectly synchronised with the grid voltage, a phase-locked loop (PLL) is utilized. The

PLL continuously provides the current grid phase θ , which is vital for achieving accurate synchronization [15]. This real-time phase θ is then combined with I_{max} to generate the three-phase current reference, a crucial step for aligning the inverter's output with the grid's requirements.

The control of the inverter's switching signals involves comparing the actual grid currents i_a , i_b , and i_c with their reference values. This comparison is managed using hysteresis controllers, which keep the grid currents within a predefined hysteresis band Δi around the reference values. By keeping the measured currents within this band, the hysteresis controllers ensure that the inverter's output remains consistently synchronised with the grid.

This synchronisation process is essential for the efficient and reliable injection of power into the grid. It minimises phase and current mismatches, thereby optimising the overall performance of the inverter and ensuring that the power delivered to the grid is both stable and efficient. This method not only enhances the operational reliability of the photovoltaic system but also contributes to the stability and quality of the power supply [16].

4. MAXIMUM POWER POINT TRACKING ALGORITHMS

A fundamental part of the photovoltaic (PV) system, the MPPT control is responsible for continuously monitoring and adjusting the system's operation to maximise power generation. In response to changing environmental conditions, the MPPT control in a single-stage topology works by regulating the PV voltage reference V_{pvref} , ensuring that the system operates at its maximum power output. However, this voltage is constrained by the following limitations [12]:

$$V_{pvref} \geq \sqrt{3} \times \sqrt{2} \times V_{grid} \quad (1)$$

4.1 Particle Swarm Optimisation (PSO)

PSO is a meta-heuristic algorithm that is inspired by the collective behaviour of animals in a flock, a phenomenon referred to as swarm intelligence [17]. This algorithm is particularly effective for tracking the Global Maximum Power Point (GMPP) because it can handle the non-linear and multimodal characteristics of the P-V curve, especially in challenging scenarios such as partial shading, where multiple peaks can occur. The algorithm relies on several individuals, called "particles," that are randomly distributed across the P-V curve [11]. These particles change their positions in search of the best personal position, and it is called P_{best} . As for the best position found by all particles, called G_{best} . This balance between personal best and global best ensures that the algorithm efficiently navigates the search space to avoid getting trapped in local maxima. The movement of each particle is determined by its current position, as defined by Eq. (2):

$$X_i^{K+1} = X_i^K + V_i^{K+1} \quad (2)$$

where, i is the particle's identifier and V_i^{K+1} is the velocity defined by Eq. (3):

$$V_i^{K+1} = wV_i^K + c_1r_1(P_{best} - X_i^K) + c_2r_2(P_{best} - X_i^K) \quad (3)$$

The inertia weight is denoted by the parameter w , which helps control the trade-off between exploration and exploitation. The acceleration coefficients are c_1 and c_2 which guide the particles towards their personal best and the global best positions. Random values r_1 and r_2 help introduce variability, allowing the algorithm to escape local optima and find the global maximum. These random values are typically within the range of $[0, 1]$ [2]. In order to find the global maximum power point (GMPP), the search for the maximum power point (MPP) during each iteration must satisfy the criteria shown in Eq. (4):

$$P(v)_i^{k+1} > P(v)_i^k \quad (4)$$

where, $P(v)_i^{k+1}$ and $P(v)_i^k$ denote the power of the PV modules associated with the X_i particle at iterations $k+1$ and k , respectively. The location of a particle in a single-stage system corresponds to the reference voltage V_{pvref} for the PV system. The adaptability of PSO contribute to its effectiveness in MPPT applications, enabling it to efficiently manage the dynamic characteristics of the P-V curve under varying environmental conditions. Furthermore, its capability to equilibrate exploration and exploitation allows PSO to escape local optima, facilitating the identification of the Global Maximum Power Point (GMPP). Figure 7 shows the flowchart of the PSO implementation steps for MPPT [10].

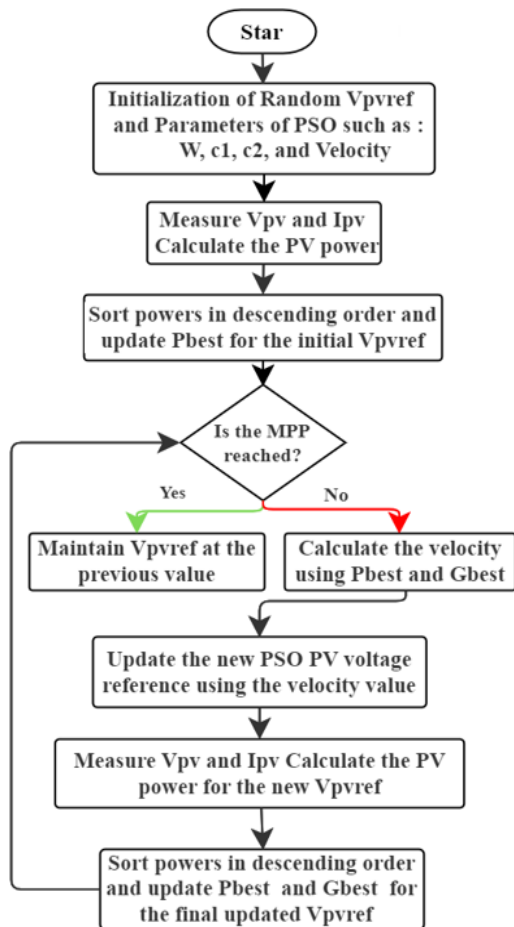


Figure 7. Flowchart of PSO

4.2 Grey Wolf Optimisation (GWO)

The social structure and hunting behaviour of grey wolves in their natural environment led one to develop the Grey Wolf

Optimisation (GWO) method. Grey wolves use a system combining α , β , δ , and ω individuals to reproduce the leadership hierarchy. This hierarchical structure is essential as it facilitates cooperative hunting, allowing wolves to efficiently locate and capture prey. We build GWO using the best appropriate solution α which precisely models the social structure of wolves. Usually indicated as β the second and third best solutions are “ δ ” accordingly. Classed as omega ω , all the other possible solutions reflect the highest negative result [18]. The process of grey wolf hunting may be divided into three distinct steps: locating, trailing, and approaching the prey; chasing, encircling, and capturing the prey; and finally, launching an assault on the prey.

The GWO implementation steps for MPPT are shown in Figure 8. The population of wolves in this optimization method is spread out randomly across the “P-V” curve, with each wolf’s position corresponding to a specific voltage value. This random distribution allows for comprehensive exploration of the solution space, which is crucial for identifying the GMPP effectively. To gauge their effectiveness, the power output of each wolf is measured, with a higher power output indicating that a wolf is closer to the Maximum Power Point (MPP). Once the wolves are ranked based on their power output, the top three are designated as α , β , and δ . These leading wolves assist in navigating the search for the MPP [19]. In contrast, the ω wolves adjust their positions by encircling the anticipated location of the MPP using the following equations:

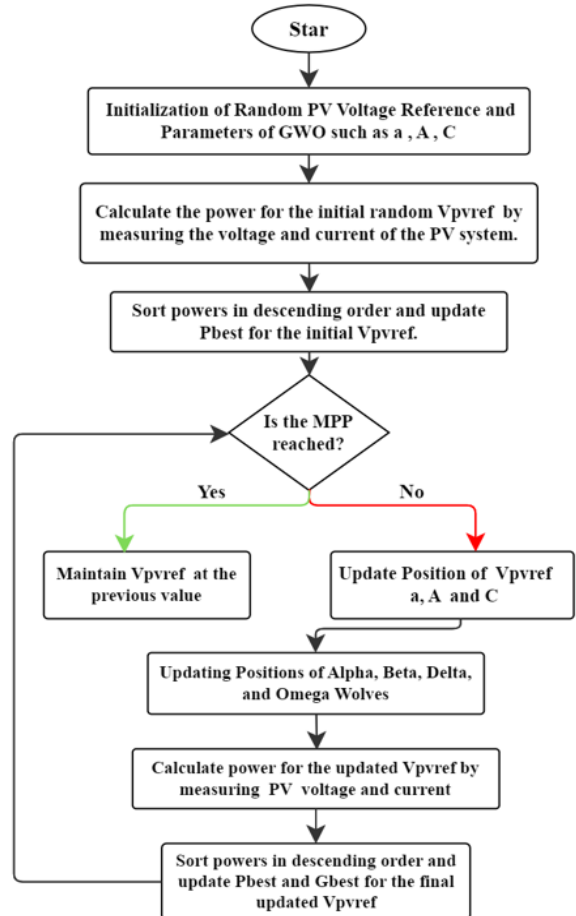


Figure 8. Flowchart of GWO

$$\vec{D} = |\vec{C}\vec{X}_p(k) - \vec{X}_p(k)| \quad (5)$$

$$\vec{X}(k+1) = \vec{X}_p(k) - |\vec{A}\cdot\vec{D}| \quad (6)$$

In this formula, K denotes the current iteration, while D , A , and C are coefficient vectors X_p represents the prey's position vector, and X is the grey wolf's position vector. The coefficient vectors A and C are calculated using the following formulas:

$$\vec{A} = 2 \cdot \vec{a} \cdot \vec{r}_1 - \vec{a} \quad (7)$$

$$\vec{c} = 2 \cdot \vec{r}_2 \quad (8)$$

The components of a decrease linearly from 2 to 0 over the course of the iterations, while r_1 and r_2 are random vectors within the range $[0, 1]$ [20]. In order to use the Grey Wolf Optimization (GWO) based MPPT in a single-stage photovoltaic system, the PV voltage is designated as the reference grey wolf. Thus, Eq. (6) can be altered in the following manner:

$$V_{pvref\ i}(k + 1) = V_{pvref\ i}(k) - A \times D \quad (9)$$

The fitness function of the GWO algorithm is defined in the following way:

$$P(V_{pvref\ i})^K > P(V_{pvref\ i})^{K-1} \quad (10)$$

5. HARDWARE DESCRIPTION, RESULTS, AND DISCUSSION OF THE SINGLE-STAGE THREE-PHASE GRID-CONNECTED PV SYSTEM

In order to empirically verify the effectiveness of the MPPT technique in a single-stage grid-connected system, a test rig was built in the LGEB laboratory. Figure 9 displays a detailed diagram of our experimental setup, comprising two photovoltaic (PV) panels connected to a three-phase inverter. The inverter is connected to the grid via a passive filter and an autotransformer. The DC sensors are used to measure the current and voltage in the photovoltaic system. These measurements are then inputted into the ADC (Analogue-to-Digital Converter) of the LAUNCHXL-F28379D. This development kit is designed to manage the process of maximum power point tracking (MPPT) and generate a PV voltage reference using its digital-to-analogue converter (DAC). The reference voltage, along with the measured voltage and current obtained from the AC sensors, is then

transmitted to the dSPACE DS1104 control board's ADC. During the final control stage, the dSPACE system utilises this data to generate six synchronised pulse (PWM) signals that drive the three-leg Gate (IGBT) grid-side inverter. In addition, a Fluke 435 power quality and energy analysers were used to guarantee efficient power injection into the grid and verify the quality of the AC power, including its total harmonic distortion (THD) and phase angle.

Figure 10 depicts the experimental test bench at the LGEB laboratory. The experiment utilised a DC link capacitor with a capacity of 2200 μ F, an L-filter with an inductance of 10 mH, and a three-phase autotransformer with a voltage rating of 21/380 V. The experiment took place on March 11, 2024, under clear weather conditions with slowly varying solar radiation. Specifically, the temperature was 32°C, and the solar irradiance was 700 W/m².

As previously mentioned, the solar panels in this study are subjected to partial shading, resulting in two local maximum power points and one global maximum power point of 191.17 W at 38.92 V, as illustrated in Figure 4. The results in Figure 11 reveal that both algorithms were effective in approaching the global maximum power point. Notably, the GWO algorithm significantly outperformed the PSO algorithm in terms of accuracy, achieving a power output of “190.12 W” compared to 188.76 W for PSO, a difference of approximately 2 W. While the difference in output power may seem minor in this experiment, its significance increases substantially in high-PV power systems, where it can become a considerable discrepancy with notable impacts on overall efficiency and energy generation. More importantly, GWO demonstrated superior speed, reaching the global maximum power point in just 2.8 s, whereas PSO required 8.8 s, resulting in a significant 6 s difference. This notable difference highlights the advantage of GWO’s advanced search techniques and its ability to adapt quickly to varying conditions. Furthermore, the simplicity of GWO's hierarchical structure allows for more efficient navigation of the solution space, in contrast to the complexity involved in managing numerous individuals within the PSO swarm, which can hinder its efficiency.

Given the negligible discrepancy in power reached (2 W) between the two algorithms, the difference in their results on the AC side, after reaching the maximum power point, is insignificant. Therefore, the remaining results equally reflect the performance of both algorithms.

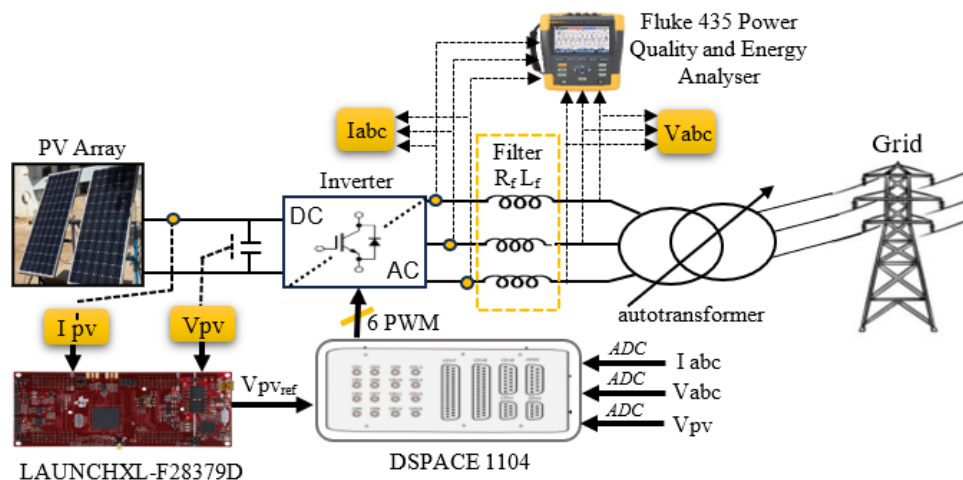


Figure 9. Experimental structure of the single-stage, three-phase grid-connected photovoltaic system

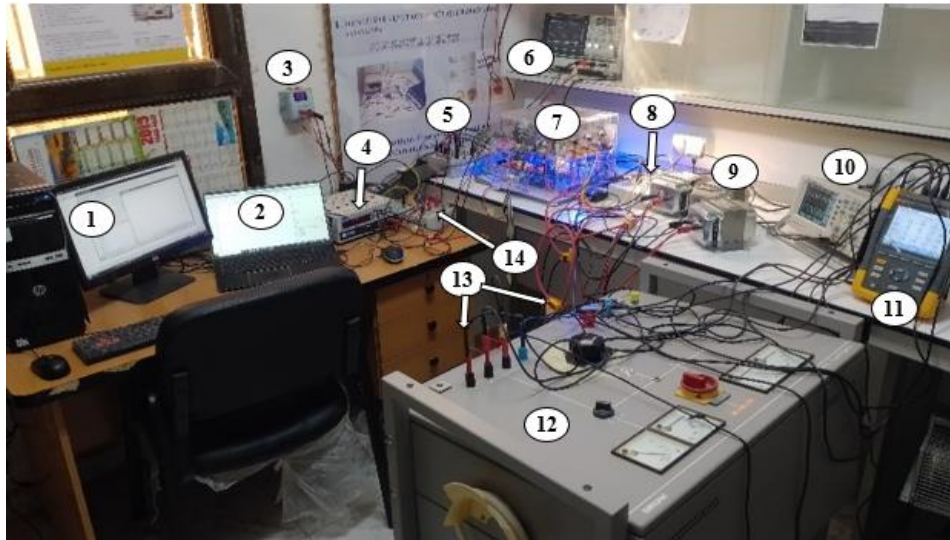


Figure 10. Laboratory equipment for experimental procedures

Note: 1. Computer for dSPACE 1104 Control. 2. Laptop for LAUNCHXL-F28379D Control. 3. Photovoltaic Panel Input. 4. Development Kit LAUNCHXL-F28379D. 5. Real-Time Hardware dSPACE 1104. 6. Oscilloscope for DC Measurements. 7. Three-Phase Inverter. 8. AC Current and Voltage Sensors. 9. Passive Filter (L). 10. Oscilloscope for AC Measurements. 11. Fluke 435 Power Quality and Energy Analyser. 12. Three-Phase Autotransformer. 13. Fluke Current and Voltage Sensors. 14. DC Current and Voltage Sensors

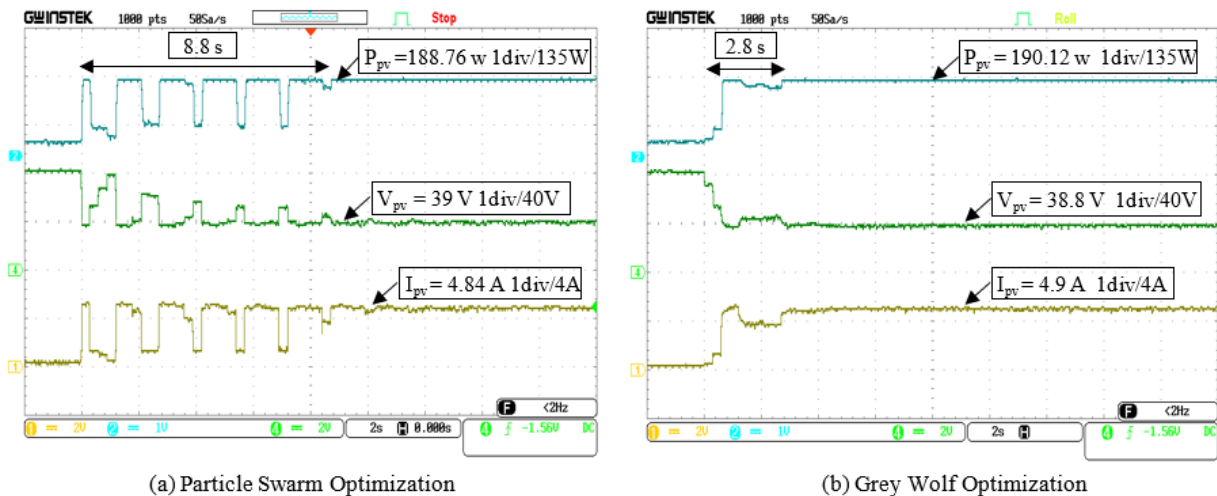


Figure 11. Experimental results for MPPT techniques

The injected current in the grid reached 4.6 A for each phase, as shown in Figures 12, 13, and 14. There is also an observed inversion in the voltage and current signals, indicating a phase angle difference of 180° , which occurs when power is injected into the grid. As shown in Figure 15, all phases are balanced with an ideal phase angle difference of 120° between the three phases' currents and a stable frequency of 50 Hz. Slight distortions in the current waveforms are likely due to harmonics introduced by the system's switching components. However, with a low total harmonic distortion (THD) of 3.7% for current and 1.8% for voltage, as shown in Figures 16 and 17, these distortions remain within acceptable limits for most industrial applications. THD values below 5% are generally considered safe and compliant with international standards [21]. This confirms the quality of the injected power and demonstrates the effective performance of the inverter control method, ensuring the stability of the single-stage system. Finally, the results in Figure 18 show that the active power injected into the grid was 170 W. Compared to the power of the solar panels, the losses in the inverter, filter resistance, wiring, and measuring devices amount to approximately 20 W,

which is a very acceptable value. Furthermore, no reactive power is injected into the grid, indicating a unit power factor, thanks to the effective synchronisation between the injected current and the grid.

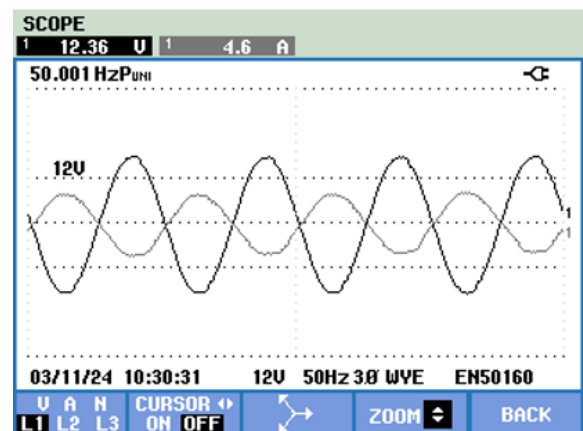


Figure 12. Voltage and current in phase 1

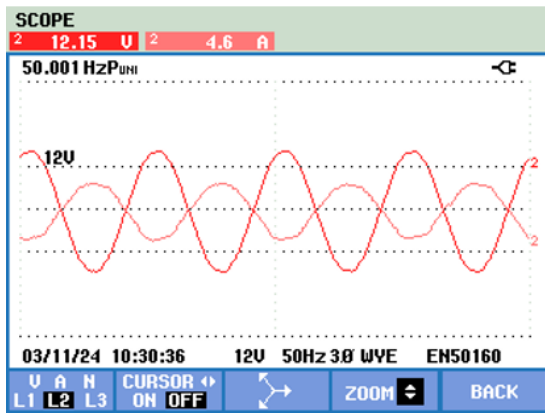


Figure 13. Voltage and current in phase 2

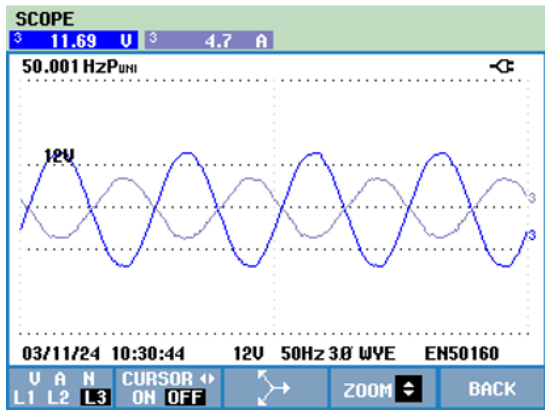


Figure 14. Voltage and current in phase 3

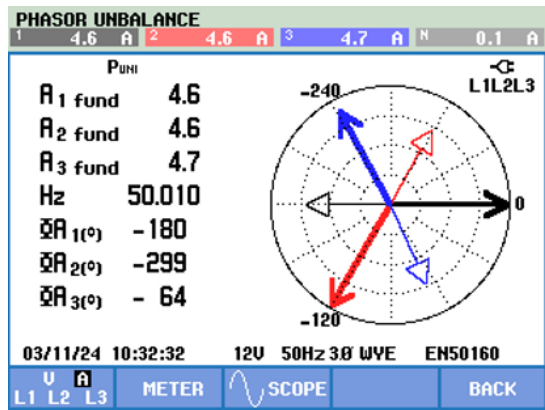


Figure 15. Phasor unbalance

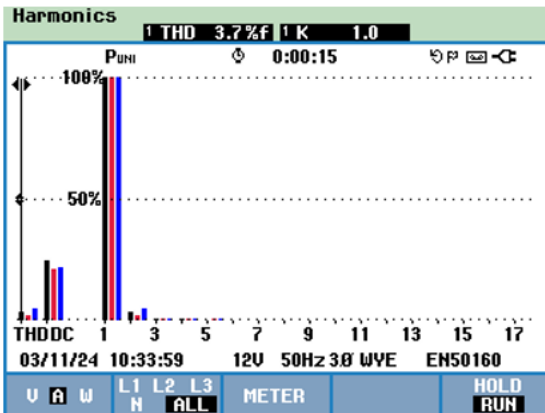


Figure 16. Current THD

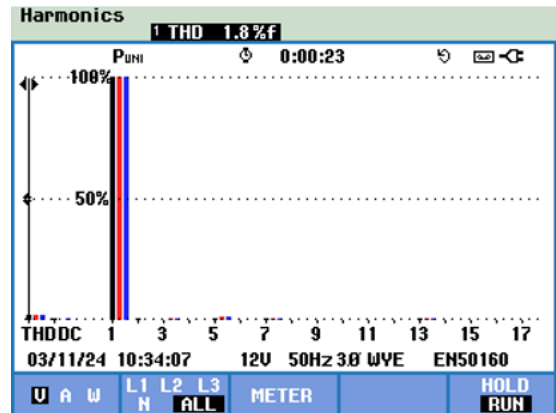


Figure 17. Voltage THD

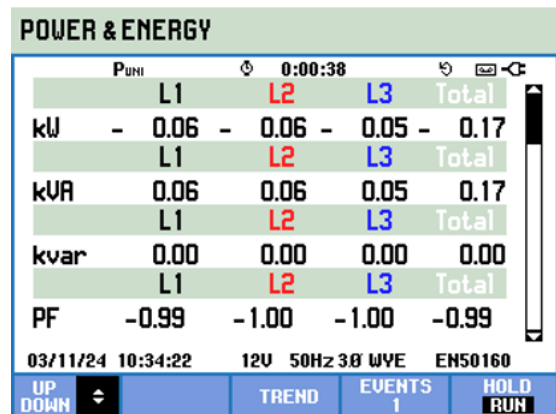


Figure 18. Injected power

6. CONCLUSIONS

This study effectively demonstrates the efficiency of optimisation algorithms for Maximum Power Point Tracking (MPPT) in partially shaded solar panels using a single-stage topology. The partial shading of the solar panels led to the emergence of two local maximum power points and one global maximum power point of “191.17 W” at “38.92 V”. In this context, the Grey Wolf Optimisation (GWO) algorithm achieved remarkable performance, reaching the global maximum power point in just “2.8 s”, whereas the PSO algorithm took 8.8 seconds. Furthermore, GWO produced a power output of “190.12 W” compared to PSO’s “188.76 W”, resulting in a difference of approximately “2 W”. This outcome highlights GWO’s superior efficiency, recorded at 99.45%, underscoring its speed and effectiveness in optimising photovoltaic power output.

During the power injection into the grid, the system successfully maintained a 120-degree phase angle difference between the currents in each phase, ensuring a stable frequency of 50 Hz. With a low total harmonic distortion (THD) of 3.7% for current and 1.8% for voltage, and without any reactive power being injected into the grid, these results emphasise the quality, performance, and stability of the single-stage system in grid-connected solar applications.

Future research could focus on evaluating these algorithms under different shading conditions to determine their adaptability and robustness. Additionally, developing hybrid PSO-GWO algorithms may leverage the strengths of both techniques, potentially leading to enhanced optimisation

results. Applying deep learning for improved accuracy and speed could enable more precise tracking of maximum power points. Furthermore, optimising inverter designs is essential for boosting efficiency, minimising losses, and improving overall system performance.

ACKNOWLEDGMENT

This work is supported by the LMSE Laboratory and the LGEB Laboratory, whose contributions were crucial for the successful implementation of the practical aspects of this project.

REFERENCES

- [1] EL-Banna, M.H., Hammad, M.R., Megahed, A.I., AboRas, K.M., Alkuhayli, A., Gowtham, N. (2024). On-grid optimal MPPT for fine-tuned inverter based PV system using golf optimizer considering partial shading effect. *Alexandria Engineering Journal*, 103: 180-196. <https://doi.org/10.1016/j.aej.2024.05.115>
- [2] Refaat, A., Khalifa, A.E., Elsakka, M.M., Elhenawy, Y., Kalas, A., Elfar, M.H. (2023). A novel metaheuristic MPPT technique based on enhanced autonomous group Particle Swarm Optimization Algorithm to track the GMPP under partial shading conditions-Experimental validation. *Energy Conversion and Management*, 287: 117124. <https://doi.org/10.1016/j.enconman.2023.117124>
- [3] Bislimi, A., Nikaj, A. (2023). Analyzing solar energy integration in smart grids with a focus on demand response, energy management, and grid stability. <https://www.researchgate.net/publication/377952692>.
- [4] Asnil, A., Krimadinata, K., Astrid, E., Husnaini, I. (2024). Enhanced incremental conductance maximum power point tracking algorithm for photovoltaic system in variable conditions. *Journal Européen des Systèmes Automatisés*, 57(1): 33-43. <https://doi.org/10.18280/jesa.570104>
- [5] Priyadarshi, N., Sanjeevikumar, P., Bhaskar, M. S., Azam, F., Taha, I.B., Hussien, M.G. (2022). An adaptive TS-fuzzy model-based RBF neural network learning for grid integrated photovoltaic applications. *IET Renewable Power Generation*, 16(14): 3149-3160. <https://doi.org/10.1049/rpg2.12505>
- [6] Nassef, A.M., Abdelkareem, M.A., Maghrabie, H.M., Baroutaji, A. (2023). Review of metaheuristic optimization algorithms for power systems problems. *Sustainability*, 15(12): 9434. <https://doi.org/10.3390/su15129434>
- [7] Moulay, F., Habbati, A., Lousdad, A. (2022). The design and simulation of a photovoltaic system connected to the grid using a boost converter. *Journal Européen des Systèmes Automatisés*, 55(3): 367-375. <https://doi.org/10.18280/jesa.550309>
- [8] Raj, S., Mandal, R.K., De, M. (2021). A single-stage three phase CT-Type MLI for grid integration and for supplying critical loads. *Journal Européen des Systèmes Automatisés*, 54(5): 713-720. <https://doi.org/10.18280/jesa.540506>
- [9] Petronijevic, M.P., Radonjic, I., Dimitrijevic, M., Pantić, L., Calasan, M. (2024). Performance evaluation of single-stage photovoltaic inverters under soiling conditions. *Ain Shams Engineering Journal*, 15(1): 102353. <https://doi.org/10.1016/j.asej.2023.102353>
- [10] Zeddini, M.A., Krim, S., Mimouni, M.F. (2023). Experimental validation of an advanced metaheuristic algorithm for maximum power point tracking of a shaded photovoltaic system: A comparative study between three approaches. *Energy Reports*, 10: 161-185. <https://doi.org/10.1016/j.egy.2023.06.019>
- [11] Houam, Y., Terki, A., Bouarroudj, N. (2021). An efficient metaheuristic technique to control the maximum power point of a partially shaded photovoltaic system using crow search algorithm (CSA). *Journal of Electrical Engineering & Technology*, 16: 381-402. <https://doi.org/10.1007/s42835-020-00590-8>
- [12] Orłowska-Kowalska, T., Blaabjerg, F., Rodríguez, J. (eds.). (2014). *Advanced and Intelligent Control in Power Electronics and Drives*. Springer.
- [13] Al-Shetwi, A.Q., Sujod, M.Z., Hannan, M.A., Abdullah, M.A., Al-Ogaili, A.S., Jern, K.P. (2020). Impact of inverter controller-based grid-connected pv system in the power quality. *International Journal of Electrical and Electronic Engineering & Telecommunications*, 9(6): 462-469. <https://doi.org/10.18178/ijeetc.9.6.462-469>
- [14] Dahmani, A., Himour, K., Guettaf, Y. (2023). Optimization of power quality in grid connected photovoltaic systems. *Journal Européen des Systèmes Automatisés*, 56(6): 1095-1103. <https://doi.org/10.18280/jesa.560619>
- [15] Luhtala, R., Alenius, H., Roinila, T. (2020). Practical implementation of adaptive SRF-PLL for three-phase inverters based on sensitivity function and real-time grid-impedance measurements. *Energies*, 13(5): 1173. <https://doi.org/10.3390/en13051173>
- [16] Hassan, S.Z., Kamal, T., Riaz, M.H., Shah, S.A.H., Ali, H.G., Riaz, M.T., Sarmad, M., Zahoor, A., Khan, M.A., Miqueleiz, J.P. (2019). Intelligent control of wind-assisted phev smart charging station. *Energies*, 12(5): 909. <https://doi.org/10.3390/en12050909>
- [17] Saadi, S.I., Mohammed, I.K. (2022). Power control approach for PV panel system based on PSO and INC optimization algorithms. *Journal Européen des Systèmes Automatisés*, 55(6): 825-834. <https://doi.org/10.18280/jesa.550615>
- [18] Almutairi, A., Abo-Khalil, A.G., Sayed, K., Albagami, N. (2020). MPPT for a PV grid-connected system to improve efficiency under partial shading conditions. *Sustainability*, 12(24): 10310. <https://doi.org/10.3390/su122410310>
- [19] Tella, V.C., Agili, B., He, M. (2024). Advanced MPPT control algorithms: A comparative analysis of conventional and intelligent techniques with challenges. *European Journal of Electrical Engineering and Computer Science*, 8(4): 6-20. <https://doi.org/10.24018/ejece.2024.8.4.623>
- [20] Sheela K,G. (2022). Metaheuristic algorithm based maximum power point tracking technique combined with one cycle control for solar photovoltaic water pumping systems. *Frontiers in Energy Research*, 10: 902443. <https://doi.org/10.3389/fenrg.2022.902443>
- [21] Menadi, A., Abdeddaim, S., Ghamri, A., Betka, A. (2015). Implementation of fuzzy-sliding mode based control of a grid connected photovoltaic system. *ISA Transactions*, 58: 586-594. <https://doi.org/10.1016/j.isatra.2015.06.009>

NOMENCLATURE

G_{best}	Global best
GMPP	Global Maximum Power Point
GWO	Grey Wolf Optimizer
I_{max}	The reference current peak value
I_{pv}	Photovoltaic panel Current
LMPP	Local Maximum Power Point
MPPT	Maximum Power Point Tracking
P_{best}	Personal best
PLL	Phase-Locked Loop
PSC	Partial Shading Condition

PSO	Particle Swarm Optimization
PV	Photovoltaic
P_{PV}	Photovoltaic panel power
V_{pvref}	Reference voltage of PV array
V_{pv}	Photovoltaic panel voltage
THD	Total harmonic distortion

Greek symbols

θ	Phase angle
----------	-------------